(4)

AD-A216 289

NUMERICAL SIMULATION OF SUPERSONIC FREE SHEAR LAYERS

ONR Contract No. N00014-89-J-1319

Semi-Annual Progress Report for the Period

June 1 , 1989 - November 30, 1989

Submitted to the

Office of Naval Research
Attn: Dr. S. G. Lekoudis
Technical Monitor

Prepared By

L. N. Sankar
Associate Professor

I. Tuncer
Post-Doctoral Fellow

School of Aerospace Engineering
Georgia Institute of Technology
Atlanta, GA 30332

December 1989

INTRODUCTION

In a pioneering experimental work, Papamoschou and Roshko studied the growth characteristics of 3-D supersonic free shear layers [Ref. 1]. One of the conclusions of their study was that 3-D supersonic shear layers asymptotically approach a growth rate equal to 30% of that of subsonic shear layers. In an attempt to explain this phenomena, a series of analytical [Ref. 2,3], experimental [~~Ref.~~ 4] and computational studies [~~Ref.~~ 5,6] have recently been carried out. Many of these studies focused on 2-D supersonic shear layers. In these studies, and in particular, studies based on stability analysis of 2-D supersonic shear layers, it was found that the shear layer growth rate approaches zero (and not the 30% observed ~~in Ref. 1~~) as the convective Mach number of the shear layer increased from subsonic and supersonic.

Several theories have been proposed to explain the discrepancies between 2-D analyses and 3-D observations. Some of the theories are:

a) Effects of 3-D disturbances and 3-D Vortical structures on Shear Layer Growth: 3-D stability analyses such as those in Ref. 7 suggest that the 3-D shear layer growth may be caused by growth of 3-D unstable modes of the shear layer. These 3-D modes contribute to the shear layer growth even as the convective Mach number increases, whereas 2-D modes become less effective.

b) Effects of Walls on the Shear Layer Growth: Tam et al. [Ref. 3] and others have studied 2-D and 3-D confined shear layers within rectangular channels. They found that the coupling between the shear layer and the acoustic modes of the channel give rise to new modes of instability, which may contribute to the growth rate of 3-D shear layers.

The objective of this research is to study the stability and growth characteristics of 3-D free shear layers through a numerical solution of the 3-D unsteady, compressible Navier-Stokes equations. A general solution procedure has been constructed that may be used to study the temporal and spatial growth of 2-D and 3-D waves, to study the effects of random initial disturbances on the

shear layer growth and to study the effects of wall on the shear layer growth. This procedure thus complements the well developed techniques of linear stability analysis, and allows one to study additional non-linear phenomena such as saturation of modes, vortex pairing phenomena etc.

The solution procedure is a straight forward extension of the 2-D compressible Navier-Stokes solver documented in Ref. 6 to 3-D compressible Navier-Stokes equations. The solution procedure is second order accurate in time, and fourth order accurate in space. The computer code has been vectorized to perform efficiently on the Cray YMP and Cray 2 class of machines, and should lend itself to efficient implementation on massively parallel machine architectures.

WORK PERFORMED THROUGH THE REPORTING PERIOD

As a first application of the 3-D shear layer analysis, the temporal growth of a shear layer confined between walls was studied. The velocity, density and temperature profiles for the mean flow was chosen to be

$$u(y) = U \tanh(y)$$

$$v(y) = 0.0$$

$$w(y) = 0.0$$

$$\rho(y) = \rho_{REF}$$

$$T(y) = T_{REF}$$

Note that this initial condition corresponds to a shear layer formed at the juncture of two parallel streams of speed U, moving in opposite directions. By changing the velocity U and reference temperature T_{REF}, the Mach numbers on either side of the shear layer, and hence the "convective" Mach number may be changed. Also note that the reference length used here is the vorticity thickness of the shear layer and equals unity. A uniformly spaced Cartesian grid of size 121 x 31 x 31 was used.

The boundary conditions are as follows. At the upstream and downstream boundaries, the flow was assumed to be periodic. The length of the domain in the x- direction was chosen to be equal to the wave length of the most amplified temporal wave as reported by Michalke, equal to 15.5. The lateral boundaries were 3 unit lengths apart, and periodic boundary conditions were applied at these boundaries as well. At the top and bottom boundaries, located +3 and -3 units away, slip boundary conditions were applied. That is, the normal component of velocity at these boundaries was zero, while the derivatives of the tangential components of velocity, the density and pressure were all set to zero.

A random initial disturbance field was next superposed on the mean flow field defined earlier. This random disturbance field was generated using a random number generator, and its magnitude at any point in the flow field was restricted to be less than 3% of the speed of sound. These disturbances were imposed on the interior nodes as well as the boundary nodes, but were confined to regions of significant vorticity in the shear layer, by multiplying the computed random disturbance by the function $[1-(y/Y)^2]$ where Y is the y- location where u(y) equals 0.25U.

Calculations are first carried out for 1000 to 2000 time steps in an inviscid mode in an attempt to let these disturbances grow to sizeable values before turning on the viscous terms. Then calculations are carried out for an additional 10,000 iterations in the viscous mode. The computed flow field is analyzed at selected time level to monitor the streamwise and spanwise vorticity fields, and to compute the average turbulent kinetic energy within the flow field. To date, calculations have been carried out for 3 convective Mach numbers, 0.2, 0.4 and 0.6.

Figure 1 shows the time evolution of the streamwise (x- component) and spanwise (y-component) of the vorticity field for M=0.2 case. It is seen that the vorticity field at initial time levels is totally random. At later time levels, organized vorticity fields begin to evolve, both for the x- and the y- component. These vorticity fields continue to change from time step to time step, and do not reach a limit cycle value. Figures 2 and 3 show the vorticity fields at later time levels for convective Mach numbers 0.4 and 0.6. Again, organized vortical structures are evident.

There is a need to analyze these vorticity fields further to see if they contain dominant 2-D and 3-D modes. It will also be useful to determine if these modes compare well with linear stability analysis, particularly during the early periods of growth.

The average turbulent kinetic energy (equal to the local turbulent kinetic energy at all nodes summed up and averaged) continues to grow with time. Figure 4 shows the normalized average turbulent kinetic energy (normalized by U) as a function of non-dimensional time (Normalized by U and vorticity thickness). It is observed that the shear layer turbulent kinetic energy growth with time slows down as the convective Mach number goes from 0.2 to 0.6. This is in agreement with stability analyses for confined and free shear layers.

WORK TO BE PERFORMED DURING THE NEXT REPORTING PERIOD

During the next reporting period, the following calculations will be carried out:

a) As stated earlier, the computed velocity and vorticity fields will be compared with 3-D stability analyses to see if these two techniques predict the same behavior for the disturbance growth in time, at least during the early periods of time.

b) The computed flow fields will be analyzed, and additional calculations will be carried out to determine if 3-D (spanwise, and oblique) modes become more important as the convective increases.

c) In cooperation with Dr. C. Tam of Florida State University, calculations are planned for a spatially growing supersonic shear layer in a rectangular channel. At the upstream boundary, 2-D and 3-D modes will be imposed on the mean flow. Their linear growth at early time levels, and any non-linear interactions between the modes and with the acoustic modes of the solid wall will be analyzed.

REFERENCES

1. Papamoschou, D. and Roshko, A., "Observations of Supersonic Free Shear Layers," AIAA paper 86-0162.

2. Ragab, S., "Linear Instability Waves in Supersonic Turbulent Mixing Layers," AIAA paper 87-1418.

3. Tam, C. and Hu, F., "The Instability and Acoustic Wave Modes of Supersonic Mixing Layers Inside a Rectangular Channnel", Jounral of Fluid Mechanics, Vol. 203, pp51-76, 1989.

4. Samimi, M., Erwin, D. and Elliott, G., "Compressibility and Shock Wave Interaction Effects on Free Shear Layers," AIAA Paper 89-2460.

5. Lele, S., "Direct Numerical Simulation of Compressible Shear Layers," AIAA ppaper 89-0374, 1989.

6. Tang, W., Sankar, L.N. and Komerath, N., "Numerical Simulation of the Growth of Instabilities in Supersonic Free Shear Layers," AIAA Paper 89-0376, To appear in Journal of Propulsion and Power, 1990.

7. Soestrisno, M., Greenbough, J., Eberhardt, S. and Riley, J., "Confined Compressible Mixing Layers: Part I. Three-Dimensional Instabilities," AIAA Paper 89-1810.

Fig 1-a

Y–VORTICITY CONTOURS

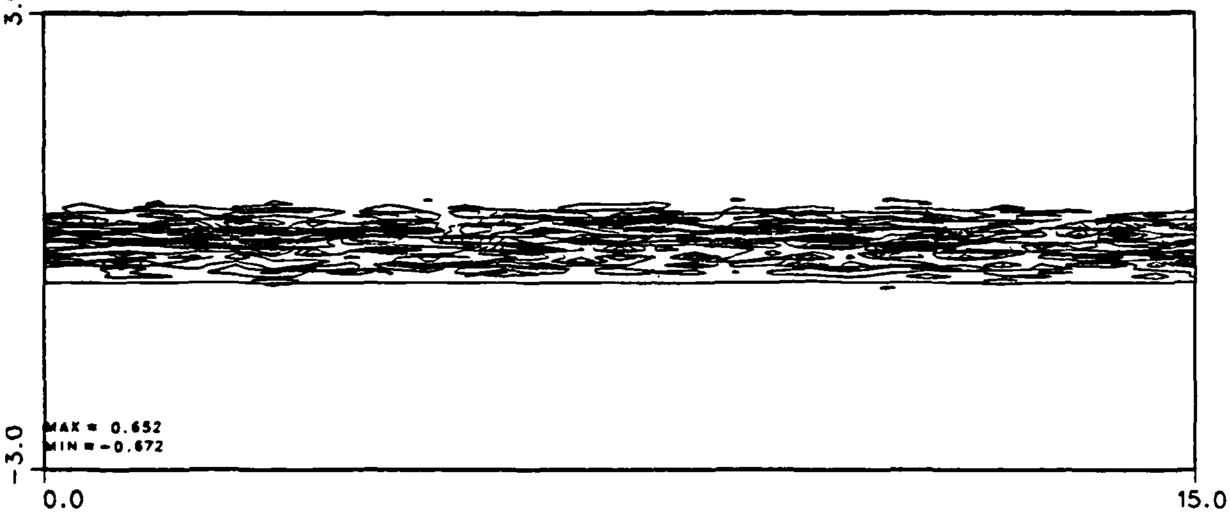

TIME STEP = 1000 STATION = 16

MACH NO. = 0.2, RE = 100.

X–VORTICITY CONTOURS

TIME STEP = 1000 STATION = 16

MACH NO. = 0.2, RE = 100.

Fig 1-c

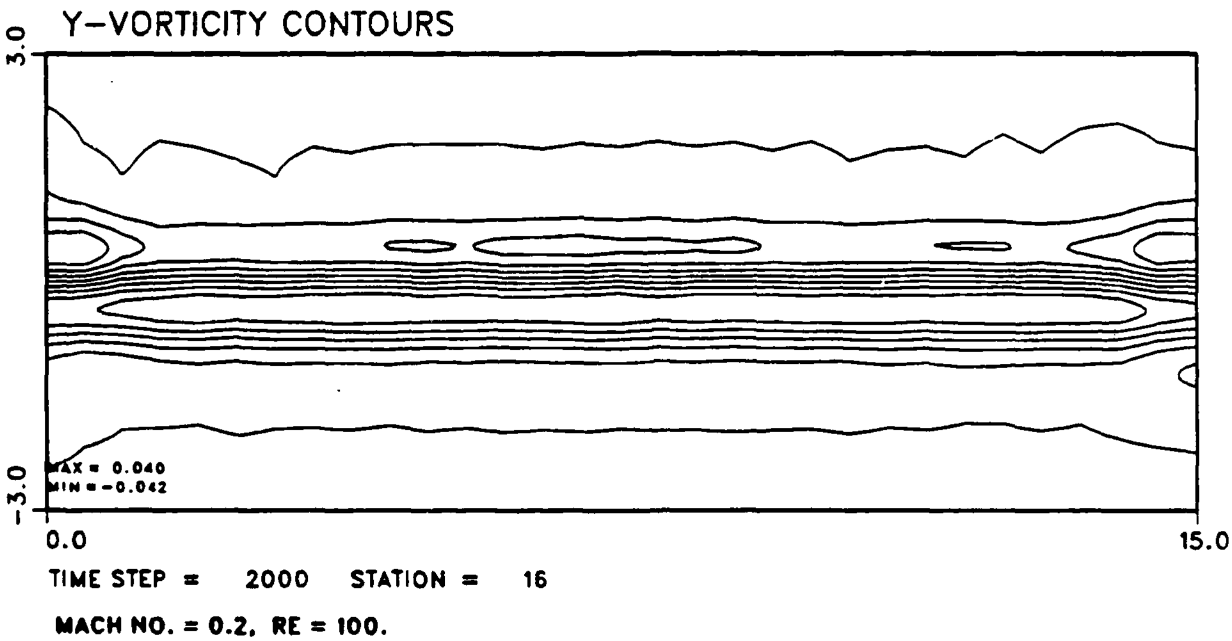
Y-VORTICITY CONTOURS
3.0
-3.0
MAX = 0.040
MIN = -0.042
0.0
15.0
TIME STEP = 2000 STATION = 16
MACH NO. = 0.2, RE = 100.

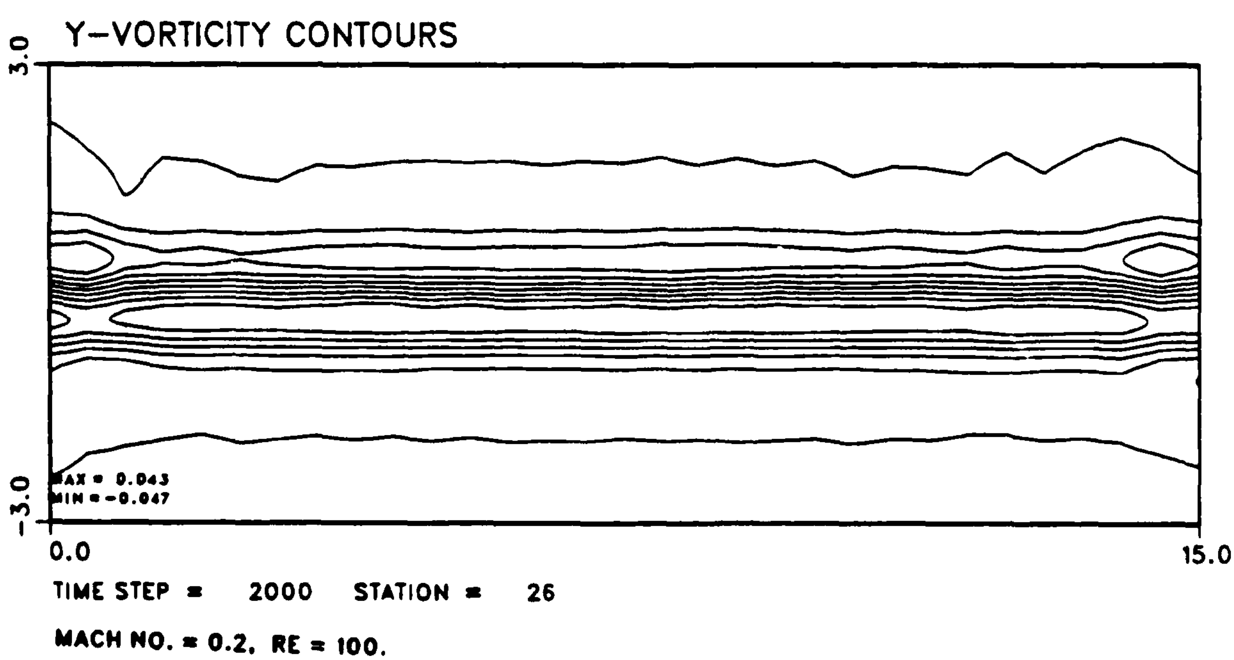
Y-VORTICITY CONTOURS
3.0
-3.0
MAX = 0.043
MIN = -0.047
0.0
15.0
TIME STEP = 2000 STATION = 26
MACH NO. = 0.2, RE = 100.

Fig 1-c

X–VORTICITY CONTOURS

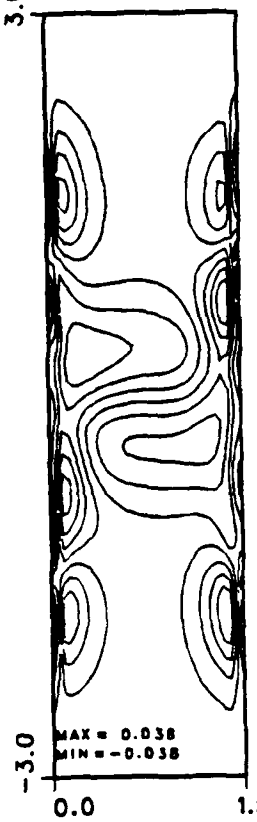

TIME STEP = 2000 STATION = 16

MACH NO. = 0.2, RE = 100.

X–VORTICITY CONTOURS

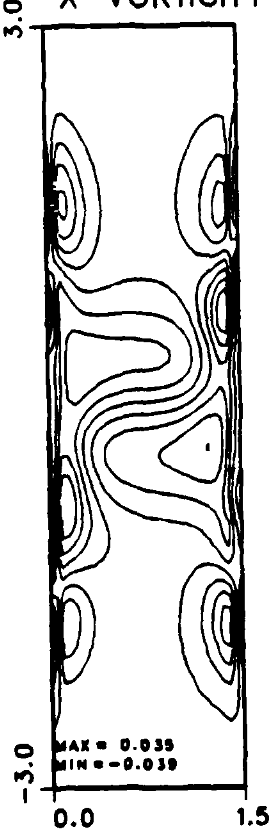

TIME STEP = 2000 STATION = 26

MACH NO. = 0.2, RE = 100.

Fig. 2-d

Y–VORTICITY CONTOURS

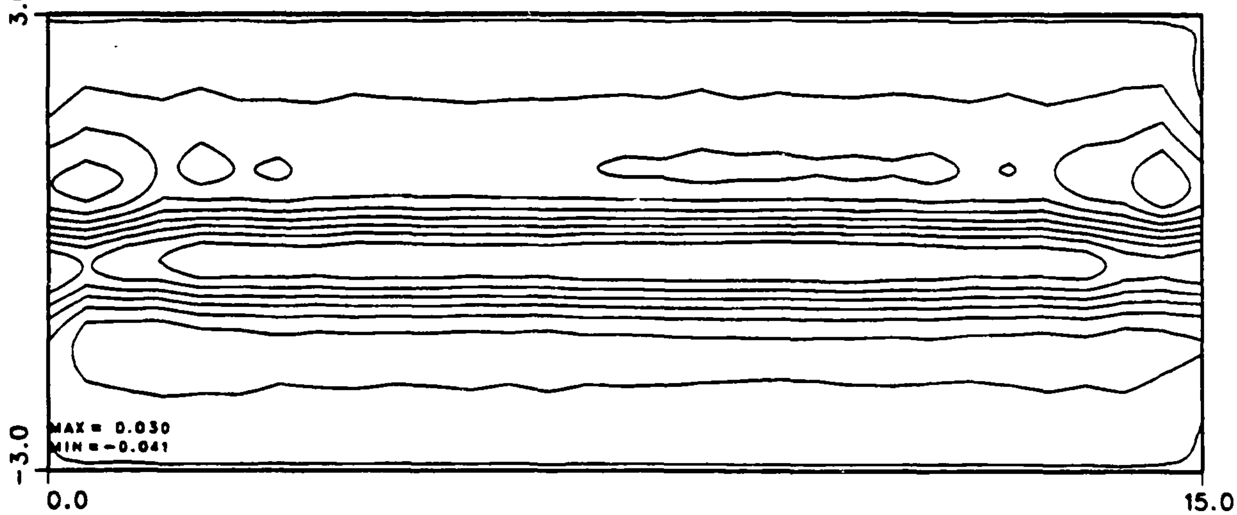

TIME STEP = 3000 STATION = 16

MACH NO. = 0.2, RE = 100.

X–VORTICITY CONTOURS

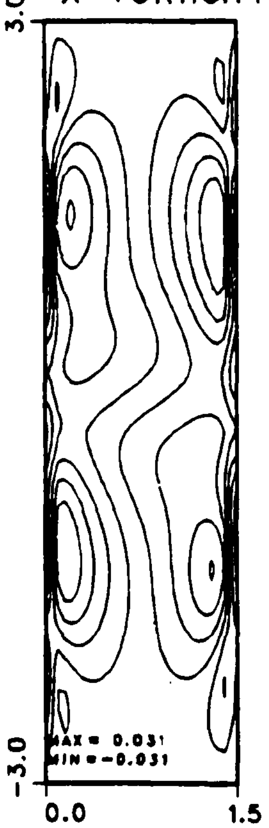

TIME STEP = 3000 STATION = 16

MACH NO. = 0.2, RE = 100.

Fig. 1-2

Y–VORTICITY CONTOURS

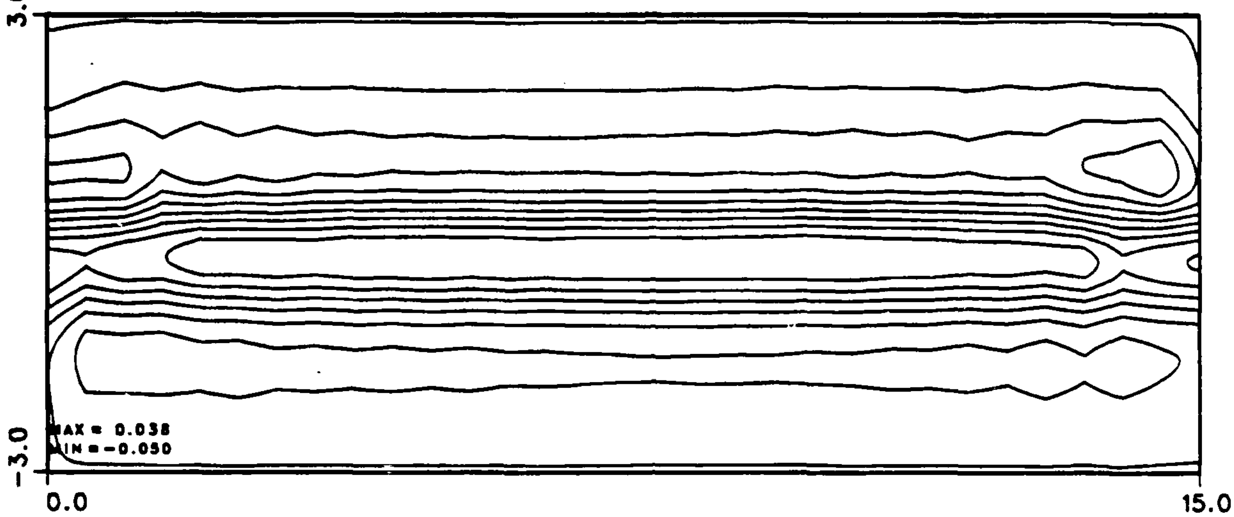

TIME STEP = 4000 STATION = 16

MACH NO. = 0.2, RE = 100.

X–VORTICITY CONTOURS

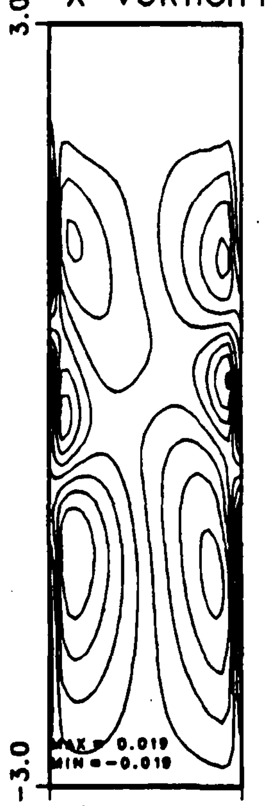

TIME STEP = 4000 STATION = 16

MACH NO. = 0.2, RE = 100.

Fig. 2-F

Y-VORTICITY CONTOURS

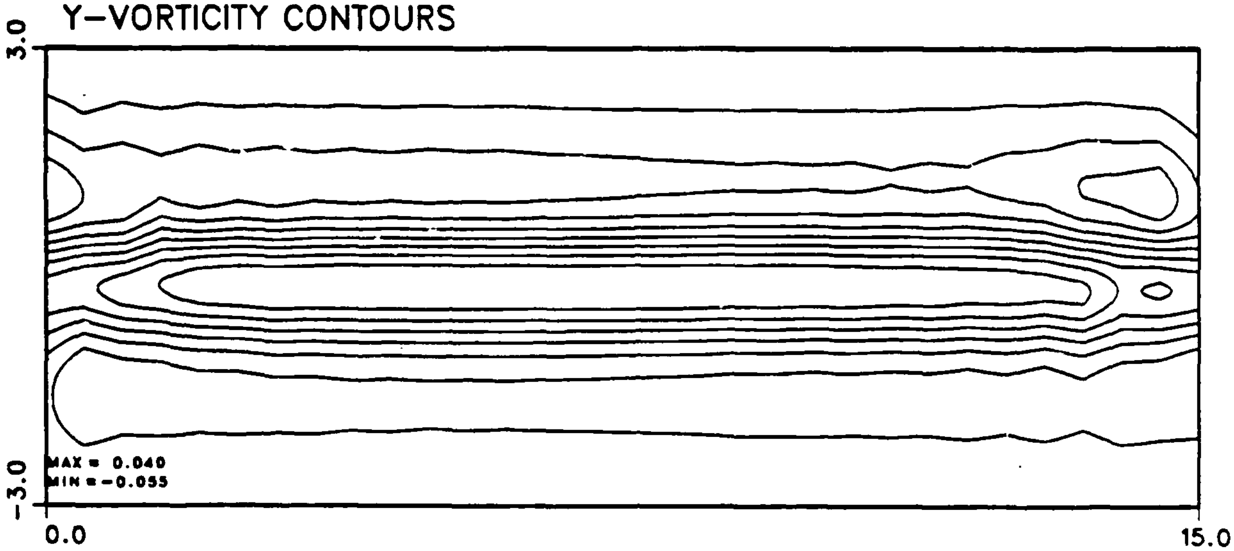

TIME STEP = 5000 STATION = 16

MACH NO. = 0.2, RE = 100.

X-VORTICITY CONTOURS

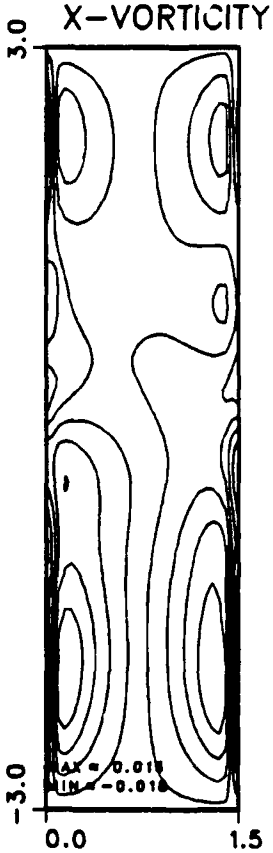

TIME STEP = 5000 STATION = 16

MACH NO. = 0.2, RE = 100.

Fig. 4-3

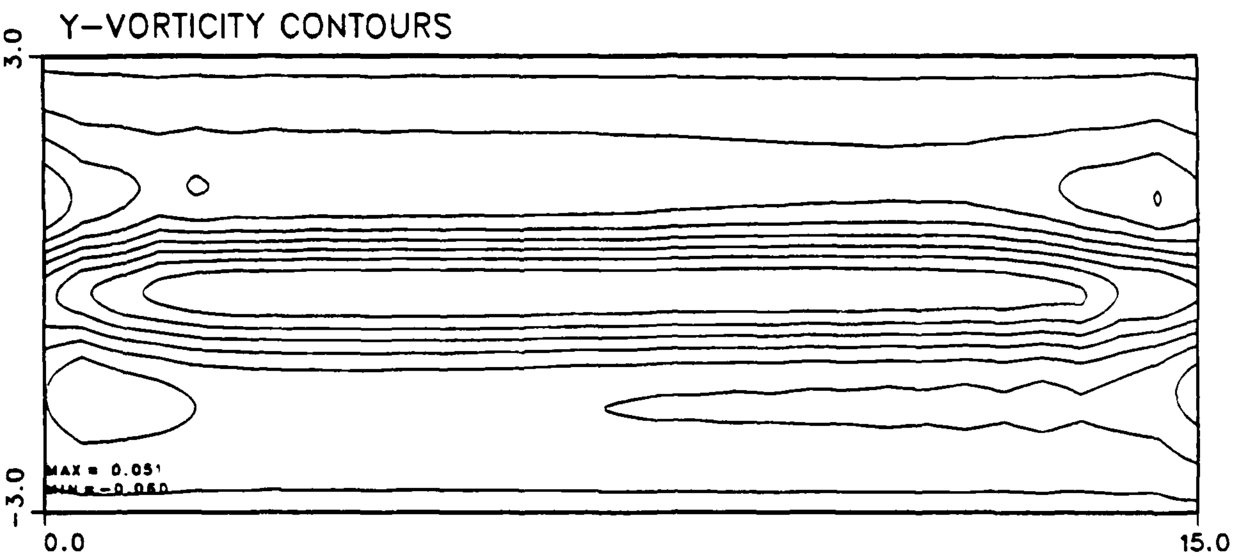

TIME STEP = 6000 STATION = 16

MACH NO. = 0.2, RE = 100.

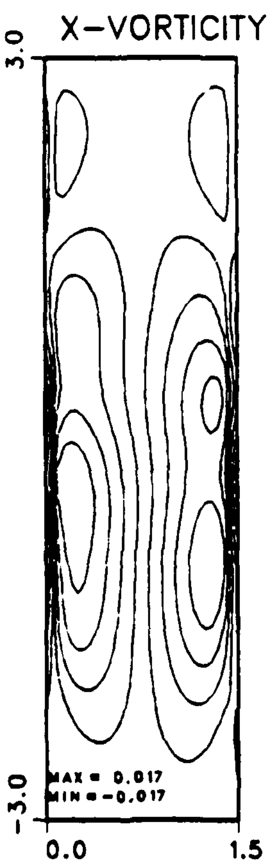

TIME STEP = 6000 STATION = 16

MACH NO. = 0.2, RE = 100.

Fig. 2-h

Y-VORTICITY CONTOURS

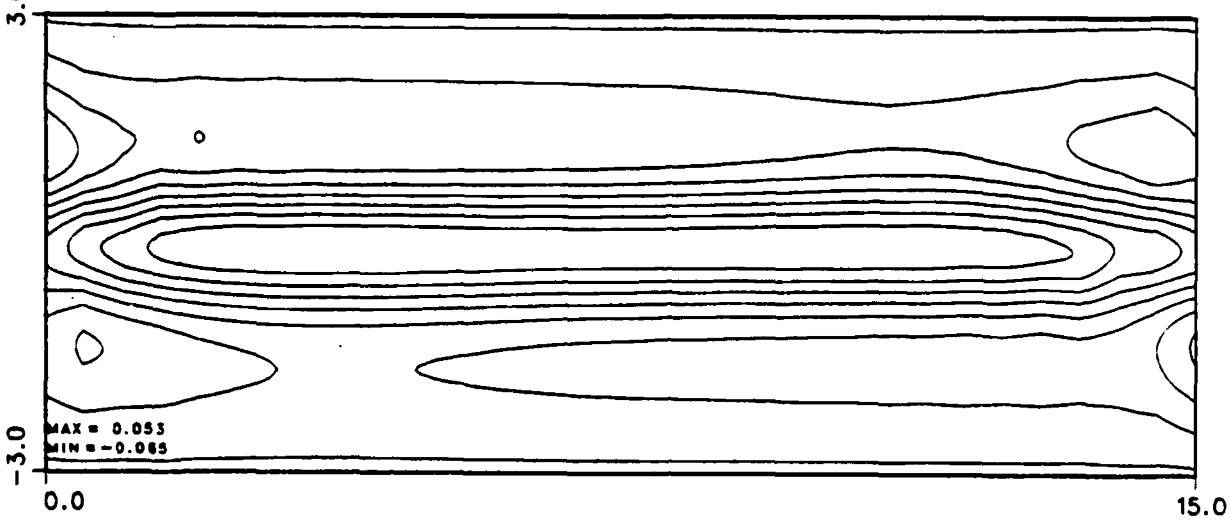

TIME STEP = 7000 STATION = 16

MACH NO. = 0.2, RE = 100.

X-VORTICITY CONTOURS

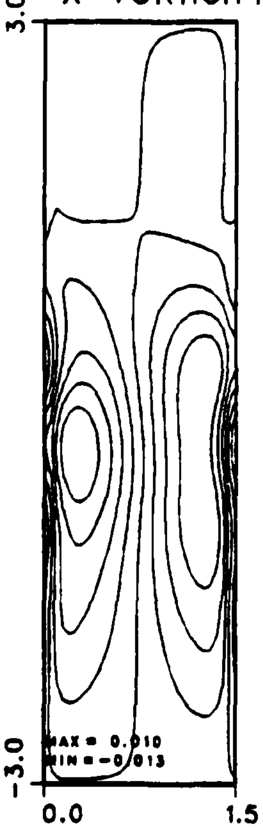

TIME STEP = 7000 STATION = 16

MACH NO. = 0.2, RE = 100.

Fig 4-2

Y-VORTICITY CONTOURS

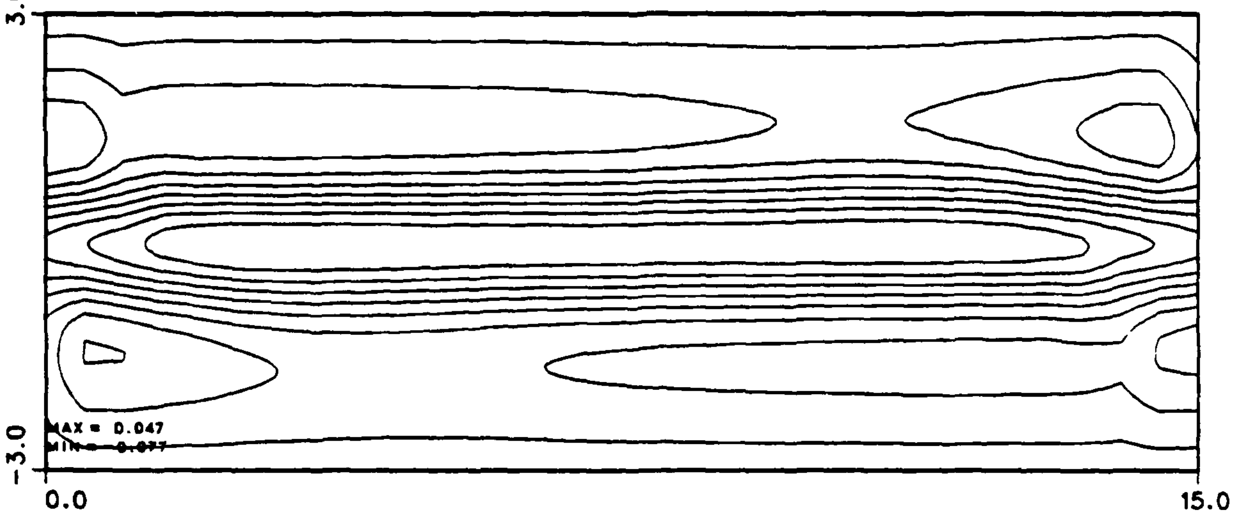

TIME STEP = 10000 STATION = 16

MACH NO. = 0.2, RE = 100.

X-VORTICITY CONTOURS

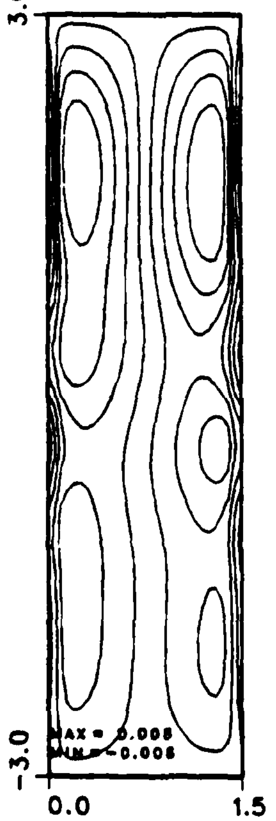

TIME STEP = 10000 STATION = 16

MACH NO. = 0.2, RE = 100.

Fig. 2-j

Y–VORTICITY CONTOURS

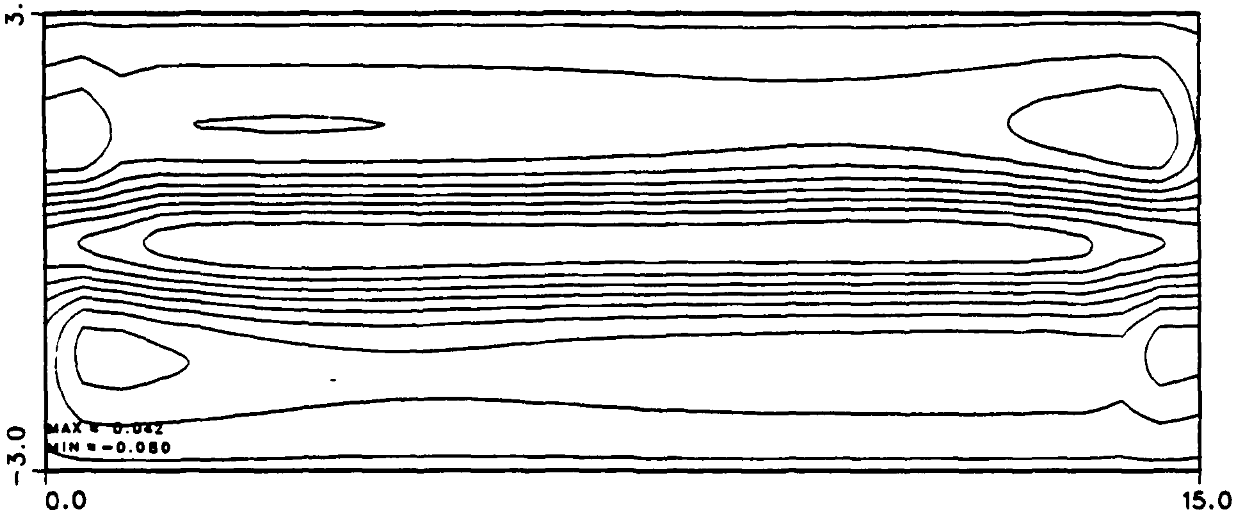

TIME STEP = 11000 STATION = 16

MACH NO. = 0.2, RE = 100.

X–VORTICITY CONTOURS

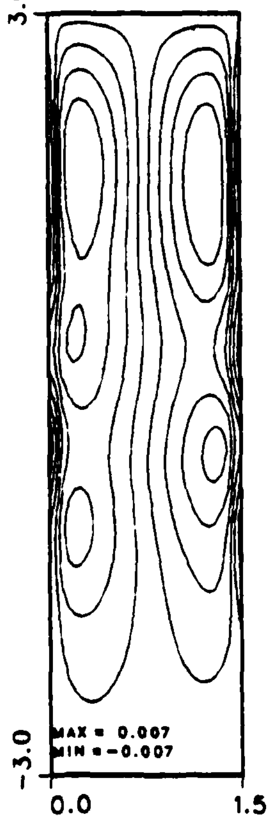

TIME STEP = 11000 STATION = 16

MACH NO. = 0.2, RE = 100.

Fig. 2

Y–VORTICITY CONTOURS

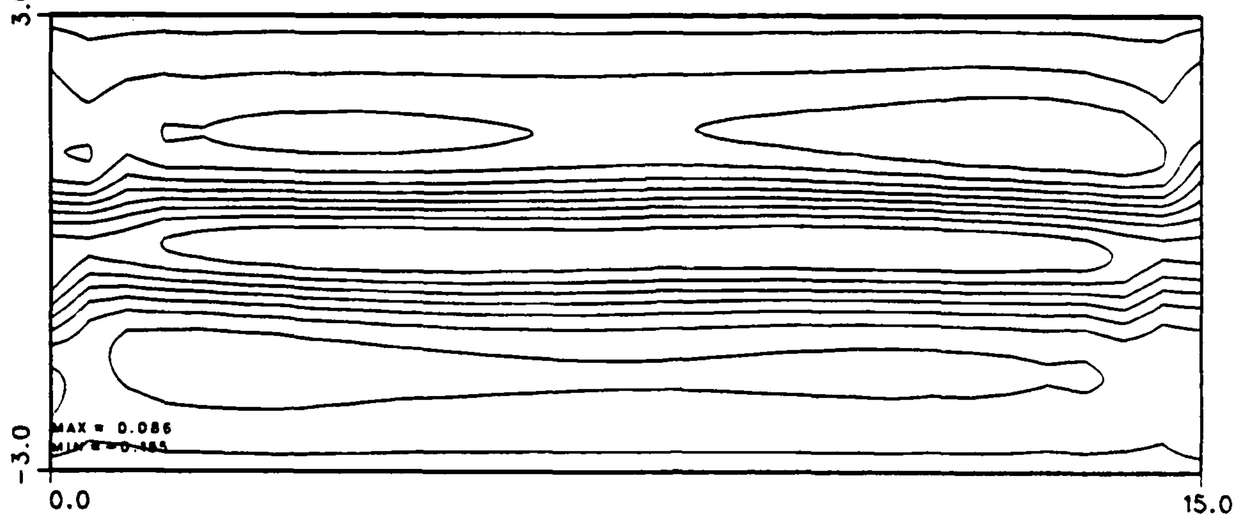

TIME STEP = 10001 STATION = 16

MACH NO. = 0.4, RE = 100.

X–VORTICITY CONTOURS

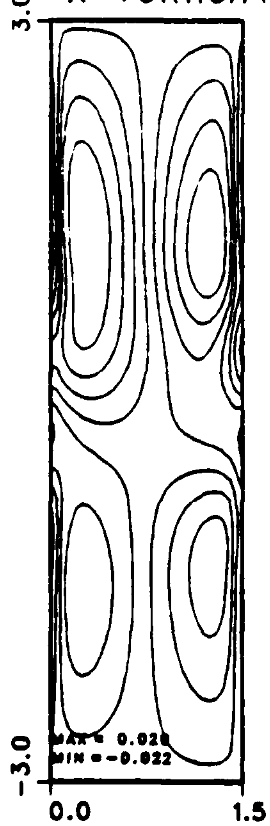

TIME STEP = 10001 STATION = 16

MACH NO. = 0.4, RE = 100.

Fig. 3

Y–VORTICITY CONTOURS

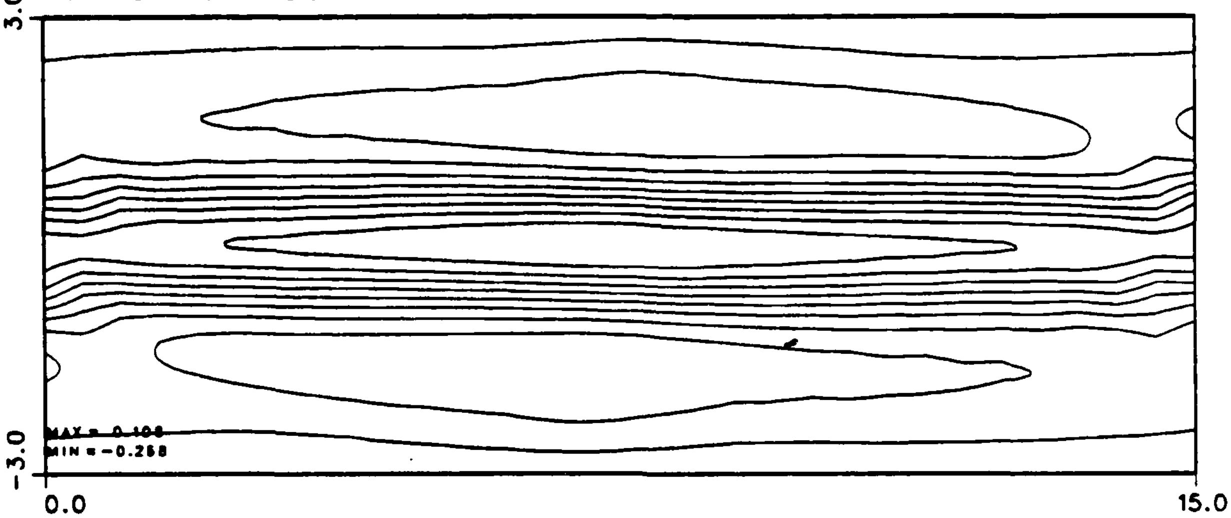

TIME STEP = 11000 STATION = 16

MACH NO. = 0.6, RE = 100.

X–VORTICITY CONTOURS

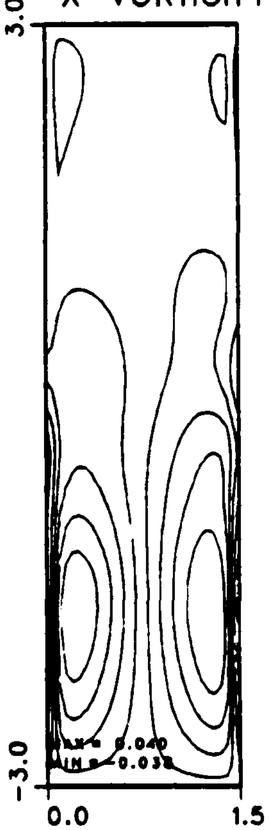

TIME STEP = 11000 STATION = 16

MACH NO. = 0.6, RE = 100.

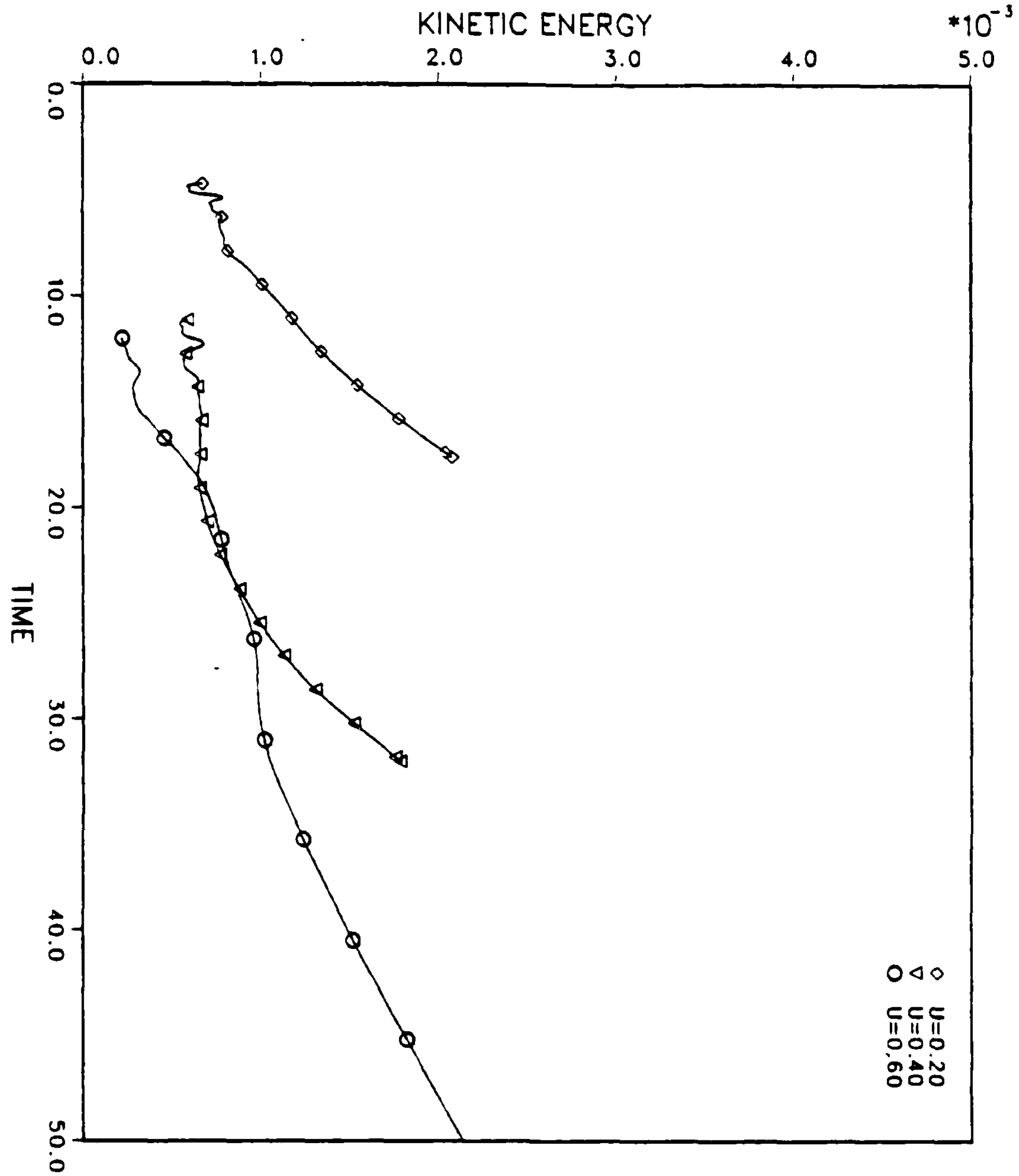
KINETIC ENERGY
*10^-3
0.0
1.0
2.0
3.0
4.0
5.0
TIME
0.0
10.0
20.0
30.0
40.0
50.0
◇ U=0.20
▽ U=0.40
○ U=0.60